ORIGINAL ARTICLE

Patterning the surface roughness of a nano fibrous scaffold for transdermal drug release

Mohammad Mahdi Saadatmand[1], Mohammad Esmail Yazdanshenas[1]*,
Ramin Khajavi[2], Fariba Mighani[3], Tayebeh Toliyat[4]

[1] *Department of Textile and Polymer Engineering, Yazd Branch, Islamic Azad University, Yazd, Iran*

[2] *Department of Polymer and Textile Engineering, South Tehran Branch, Islamic Azad University, Tehran, Iran*

[3] *Associate Professor of Weed Research Department, Iranian Research Institute of Plant Protection, Tehran, Iran*

[4] *Department of Pharmaceutics, Faculty of Pharmacy, Tehran University of Medical Sciences, Tehran, Iran*

Abstract

The main objective of this paper was to manipulate the Nano Fibrous Scaffold "NFS" surface roughness to achieve a new transdermal drug release profile. To assess the intrinsic mechanical properties of Nylon 6 or polycaprolactam, such as its proper resiliency, it was considered as the matrix. Cetirizine was used as a drug model and was loaded (1% w/v) to polymer solution (30%w/v) before spinning. Two polymeric meshes with different orifices in size and geometry were used to induce roughness on the surface of two collecting NFS during the electrospinning process. They were placed in line of conventional electrospinning, here after called "Mesh Electrospinning" and hereby, two roughened NFS were fabricated: Pentagonal templated nanofibrous scaffold (PeTNFS) and tetragonal nanofibrous scaffold (TeTNFS) beside ordinary NFS (ONFS). The kinetic of drug release was compared with known models and the release of cetirizine from these new drug delivery systems was done by UV–VIS spectroscopy and its *in-vitro* release profile was measured using Franz cell diffusion system. Release profiles from NFS were compared with a commercially available drug delivery system. To assess the simulation of NFS effect on the skin, NFS was placed on layer of dialysis film, and after three hours, the morphology was investigated using SEM. PeTNFS sample showed the greatest trend of drug release and it was about 20% more than un-roughened NFS. The best fit for drug release kinetic of NFS and TeTNFS samples were Higuchi model but it obeyed first order model for PeTNFS sample. The obtained NFS showed high potential for transdermal drug release.

Keywords: *Drug release, Franz cell diffusion, In-vitro, Mesh electrospinning, Transdermal.*

INTRODUCTION

Different methods such as solvent casting, particulate-leaching techniques, gas foaming, phase separation, porogen leaching, fiber mesh, fiber bonding, self-assembly, rapid prototyping, melt molding, membrane lamination, freeze drying, and electrospinning are employed to fabricate scaffold [1]. Electrospinning is a versatile method for spinning various polymers into nanoscale fibers [2]. Under the influence of an electric field, a pendant droplet of the polymer solution at the spinneret is deformed into a conical shape. The earliest set up of electrospinning used auxiliary electrodes to direct the electrospinning jet onto rotating collectors [3]. The principle of electrospinning involves formation of a charged jet of polymeric solution by the application of an electric field. As the jet travels in the air, the solvent evaporates, and a charged fiber left behind which can be collected on a grounded plate (collector). Electrospinning yields

* Corresponding Author Email: *dr.yazdanshenas@gmail.com*

mostly nonwoven fiber mats having large surface to volume ratios and various fiber morphologies and geometries [4]. The main parameters which affect and/or control the process of electrospinning and subsequent fiber morphology can be as follows: solution concentration, polymer molecular weight, viscosity, conductivity, surface tension, applied voltage, distance of source electrode from the target substrate, electric field, and solution flow rate [5]. Electrospun membranes have been use in various areas such as sensors, drug delivery, tissue engineering, etc. However, while producing nanofibers, the environmental conditions (temperature and relative humidity) are strongly influencing the obtained fiber morphology [6]. Among the various potential applications, drug delivery is one of the most promising uses. The high loading capacity, high encapsulation efficiency, simultaneous delivery of diverse therapies, ease of operation, and cost effectiveness are appealing features for electrospinning used in drug delivery [7-8]. From the first study on the application of electrospun nano-fibers for the sustained release of a model drug tetracycline hydrochloride using poly (lactic acid) and poly (ethylene-co-vinyl acetate), as well as their blend as polymeric matrices by Kenawy *et al.* [9], electrospun nanofibers have been successfully used to achieve different controlled drug release profiles, such as immediate, smooth, pulsatile, delayed, and biphasic releases [10-11]. And drugs ranging from antibiotics and anticancer agents to proteins, aptamer, DNA, and RNA have been incorporated into electrospun fibers [12].

Scaffolds play an important role in regenerative medicine as they can act as not only a substrate for supporting cell growth, forming certain structures, or regulating cell behaviors but also as a sustained local delivery system for growth factors and/or signaling molecules and the enhancement of cell functions and tissue regeneration. Electrospinning offers a cost-effective method for fabricating nanofiber scaffolds to mimic native ECM composed of an interlocking mesh of proteins and glycosaminoglycans. PCL, poly(lactic acid) (PLA), poly(glycolic acid) (PGA), poly(lactic-*co*-glycolic acid) (PLGA) and poly(lactic acid-*co*-caprolactone) (PLCL) are the most popular raw materials due to their ease of processing, stable mechanical properties, and good biocompatibility [13-14]. Natural polymers, such as collagen, gelatin, chitosan, and silk fibroin have also been electrospun into nanofiber scaffolds [15-17]. The ideal wound dressings should be multi-functional: fighting against acute or chronic infection; maintaining a balanced moisture and gas exchange environment; absorbing extrudates and blood from wounds; and promoting cell proliferation and migration and, thus, wound healing [18-19]. Electrospun nanofibers as wound dressings could simultaneously present all these features. The small pore size of electrospun nanofiber dressings, below 1 μm, protects the wound from bacterial penetration via aerosol particle capturing mechanisms, while allowing O_2 permeability [18]. Recent studies have demonstrated that a biosensor made of electrospun nanofibers is even capable of detecting circulating tumor cells (CTC) [20]. For example, Tseng's group developed "NanoVelcro" chips that can identify and isolate single-CTC by conjugating streptavidin and biotinylated capture agents to electrospun PLGA nanofibers [21-22]. Electrospun nanofibers have been used as a vehicle for local drug delivery due to the ease of encapsulation of chemical and biological molecules during electrospinning process. In applications of electrospun nanofibers in regenerative medicine and wound dressings, therapeutic agents are often incorporated to the nanofibers for controlled release. The ideal nanofiber formulations for drug delivery to patients should be spatially and temporally controlled. Nanofibers are often administrated in a dosage form via a local delivery route. Thus, the release of drugs occurs only at the targeted site, avoiding systematic exposure of the drugs. The spatial control of drug delivery can be readily realized by placing electrospun nanofibers at the site through invasive or non-invasive means. In earlier studies, the temporal control of drug release from electrospun nanofibers has been mainly determined by drug diffusion rates, drug dissolution rates, drug physical desorption rates, diameters of fibers (lengths of diffusion barrier), and/or polymer degradation/erosion rates [23-25]. Recent efforts have been devoted to development of activation and feedback factors electrospun nanofibers to initiate the release and/or regulate the release rate of drugs over time. Such nanofibers are also called smart electrospun nanofibers [26-27].

The objective of this study is to provide a method for modifying the surface of the electrospinning layer, to increase the amount of drug release to the skin surface; by using a rugged surface in the collector, nanofibrous scaffold with roughness was created. Articles on creating roughness on the surface of electrospun layers were included.

Conductive collecting substrate with textured surface such as wire mesh or grids was used to form patterned/textured nanofibrous membrane due to its electric field profile [28]. Electrospinning jet using polycaprolactone solution was able to detect conductive lines with width of 350 μm and spacing of 1.7 mm [29]. Grids made of parallel wires close to one another has been shown to form dense, aligned nanofibers between the wires, while a substrate with arrayed pins gave rise to membrane made of radiating nanofibers between the pins [30]. More grids variations such as having a pin in the center of a round space formed a pattern where fibers radiate from the central pin to the edges [28]. Patterned nanofibrous mesh was tested for some applications. Cell culture, as compared to proliferation of mouse osteoblastic cell between patterned/textured nanofiber and randomly oriented nanofiber, showed faster proliferation on the textured nanofiber membrane. However, initial cell adhesion is better on randomly oriented nanofiber membrane [31].

According to the above literature researches, a non-conductive mesh has not been used to make pattern on electrospinning layer yet. This study aimed to fabricate NFS with an innovated electrospinning method called "Mesh electrospinning". Two non-conductive meshes with different patterns were used in mesh electrospinning method to produce different patterned surface with different morphology and different roughness: one mesh with pentagonal meshes and the other one with tetragonal meshes (PeTNFS and TeTNFS, respectively). The spinning solution was prepared by dissolving 1.5 g nylon 6 in 5^{cc} formic acid (30% w/v). The required amount of drug (1% w/v) was added to this solution just before electrospinning. Data from our previous study [32] was also used in this experiment. Briefly, the voltage, distance and feed rate were chosen as 20 kV, 5 cm and 0.2 ml/h, respectively. After electrospinning, at first,

the surface roughness of samples was measured. The nanofibrous scaffolds were used for *in-vitro* transdermal drug release test on dialysis film by Franz diffusion cell and spectrophotometric method was used to determine the amount of drug released in phosphate buffer saline in pH 7.4 [33]. Also, the maximum wavelength absorbance of cetirizine was determined, and drug release kinetics was investigated. To simulate NFS effect on skin, NFS layers were placed on dialysis film, and after three hours, the morphology of the skin was investigated using SEM. Finally, statistical analysis was done.

EXPERIMENTAL
Material
High molecular weight Nylon 6 (63,000 g/mol) was purchased from BASF. Formic acid ACS reagent grade was purchased from Merck. Other chemicals: cetirizine dihydrochloride, European Pharmacopoeia (EP) ($C_{21}H_{25}ClN_2O_3 \cdot 2HCl$, molecular weight 461.81), potassium phosphate monobasic (KH_2PO_4, molecular weight 136.09) and sodium hydroxide 98% (NaOH, molecular weight 40) were purchased from Sigma–Aldrich, USA.

Spinning solution
The pinning solution was prepared by dissolving 1.5 g nylon 6 in 5^{cc} formic acid (30% w/v). The required amount of drug (1% w/v) was added to this solution just before electrospinning.

Scaffold fabrication (electrospinning)
The data from our previous study [32] was also used in this experiment. Briefly, the voltage, distance and feed rate were chosen as 20 kV, 5 cm and 0.2 ml/h, respectively. The model of electrospinning unit was DAIWAHA, Korea**.** Two patterns of meshes as shown in Fig. 1 were used: one with pentagonal meshes (Fig. 1a), 66.75% free area and a mesh of 7 (cm^{-1}); the other one with
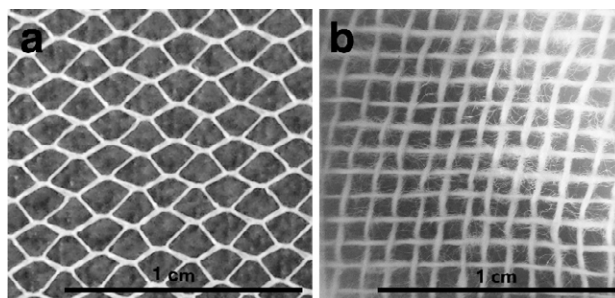

Fig. 1. Pattern of meshes and roughness on electrospun layers (a: Pentagonal; b: Tetragonal).

Table 1. Roughness of samples.

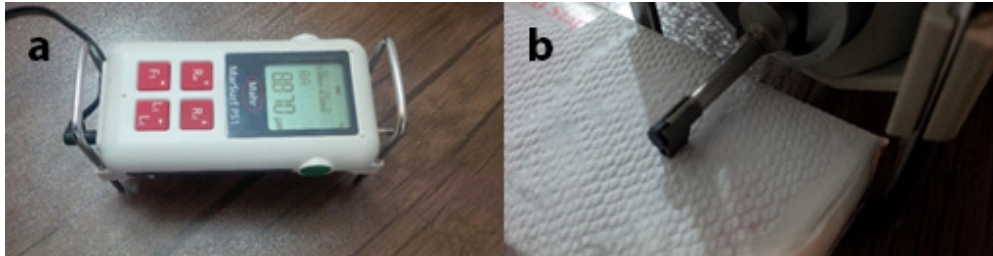| Sample:	ONFS	PeTNFS	TeTNFS
R_a (µm):	0.814	4.163	2.292
R_z (µm):	9.56	18.3	12.6

Fig. 2. a: Roughness Tester (MarSurf PS1), b: Moving probe on the sample surface.

tetragonal meshes (Fig. 1b), 33.375% free area and a mesh of 9.5 (cm^{-1}).

Three nanofibrous layers were fabricated:

Ordinary nanofibrous scaffold (ONFS), pentagonal templated nanofibrous scaffold (PeTNFS) and tetragonal nanofibrous scaffold (TeTNFS).

Drug Release Trend

First, the maximum wavelength absorbance of cetirizine was determined. An aqueous solution with 100 µg/ml of cetirizine was prepared and its absorbance on different wave numbers was determined with UV-VIS Spectro Photometer (Mexasvs, Korea). Then, the standard curve of cetirizine was shown. To obtain calibration curve, some stock solutions with concentration of 2.5, 5, 10, 15 and 20 µg/ml of cetirizine were prepared, and their absorbance measured on obtained λ_{max} of cetirizine. The standard curve was plotted in the range of 2.5-20 µg/ml, and the equation for the best fitted line was obtained (y= mx+c). Finally, the drug release trend of different samples was determined in buffer phosphate sodium (BPS) at different times (45-165 min).

Roughness test

The roughness of surface samples was measured by Mobil Roughness Tester (Mahr, MarSurf PS1, Germany). Stylus tip was 2 µm and pressure force was averagely 0.7 mN. Measurement scanning length was adjusted as 17.5 mm. MarSurf PS1 portable surface roughness device was first used for measurement by moving probe on the sample surface through a 17.5 mm length and this device automatically calculated R_z and R_a [32]. Three measurements for each workpiece surface

roughness were done and averaged for each test. The results are shown in Table 1. The shape of roughness tester device shown in Fig. 2a, and its probe are shown in Fig. 2b.

Analysis Drug release kinetics data

To analyze the in-vitro release data various kinetic models were used to describe the release kinetics. The zero-order rate Eq. (3) describes the systems where the drug release rate is independent of its concentration [34]. The first-order Eq. (4) describes the release from system where release rate is concentration dependent [35]. Higuchi described the release of drugs from insoluble matrix as a square root of time dependent process based on Fickian diffusion Eq. (5) [36].

$$C = k_0 t \qquad (1)$$

Where, K_0 is zero-order rate constant expressed in units of concentration/time and t is the time.

$$LogC = LogC_0 - kt / 2.303 \qquad (2)$$

Where, C_0 is the initial concentration of drug and K is first order constant.

$$Q = Kt^{1/2} \qquad (3)$$

Where, K is the constant reflecting the design variables of the system

In-vitro release study (Franz cell diffusion)

The Franz Cell chamber is an *in-vitro* skin permeation assay (Fig. 3), and the cell was used to determine the rate of drug release from
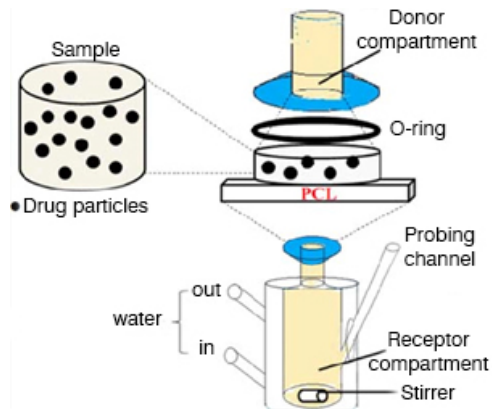
Fig. 3. Franz cell diffusion [37].

nano-fibers web produced [37]. Phosphate buffer solution (PBS) was used as the phase receptor. The Franz Cell apparatus consists of two primary chambers separated by a membrane. Although, animal skin can be used as the membrane, human skin is preferable. But due to the problem of access to human or animal skin, fluctuations due to skin type, sampling location, gender and age of animal or human, the use of synthetic membranes is common and acceptable. Cellulose dialysis film is one of the most important membranes used for this kind of study [38]. To prepare the dialysis film (molecular weight cut-off 14000 was purchased from Sigma–Aldrich, USA), it must be soaked water (at 5°C) for 24 h.

Sample was 2.5 cm in diameter and the thickness of these samples was almost constant (100 μm). Then, the weight of each sample was measured accurately with scales. To determine the amount of released drug, the test product was applied to the membrane via the top chamber. The bottom chamber contains 25 ml PBS solution with pH=4.7 for analysis and placed on a magnetic stirrer with a heater. The chamber was maintained at a constant temperature of 37°C. 45 min from the start of the experiment, samples were taken at a specified interval (every 15 min) from the receptor phase for 165 min. According to the standard curve of cetirizine and initial weight, the amount of released drug in the solution (due to the release of the drug from the nanofiber tissue) can be calculated. Finally, the drug release diagram based on time was plotted.

Simulation of NFS effect on skin:

For this experiment, NFS was placed on dialysis film and after three hours, the morphology of the skin was investigated using SEM.

Statistical Analysis

All statistical analyses were performed using the SPSS statistical software program and ANOVA test was used for measurement. In this section, due to the repetition performed at different times, the condition of independence between communities was not established; therefore, a repeated measurement test was used. At first, Mauchly's sphericity test was used. In this method, SPSS software was used to calculate the variance-covariance matrix, and then, the Mauchly's sphericity test-uniformity test for variance-covariance was performed to consider the establishment of F statistics.

RESULTS AND DISCUSSION

Morphology and roughness of samples

For electrospinning, the meshes must be fixed near the collector. Three electrospinning layers were fabricated: ONFS, PeTNFS and TeTNFS. Camera capture and their SEM images for three samples are shown in Fig. 4, which images for ONFS, PeTNFS and TeTNFS layers are shown in Fig. 4a, 4b and 4c respectively. (Scanning Electron Microscopy, JEOL, JSM-840, Japan) and the result of roughness test is shown in Table 1.

The roughness value for samples ONFS, PeTNFS and TeTNFS was 0.814, 4.163 and 2.292 μm, respectively.

Result of Drug Release Trend

The absorption spectrum of cetirizine in 200-300 nm was measured and the result is shown in Fig. 5.

The absorption spectrum showed two distinct peaks, including 212 and 231 nm. According to the history [39-40], λ_{max}=231 nm.

To determine the standard curve of cetirizine, the absorbance of the subsequent solution was measured in λ_{max} of cetirizine (231 nm). The standard curve was plotted in the range of 2.5-20 μg/ml and regression coefficient and equation for straight line was obtained. The standard curve for absorbing cetirizine is shown in Fig. 6 and standard curve of cetirizine was obtained (Equation 4). According to the correlation coefficient (R^2 = 0.999), the standard curve was acceptable.

$$y= 0.0312 \, x - 0.0317 \tag{4}$$

In-vitro Release Results

Due to the absorbance results of *in-vitro* test using Franz cell (Fig. 7) and cellulose acetate
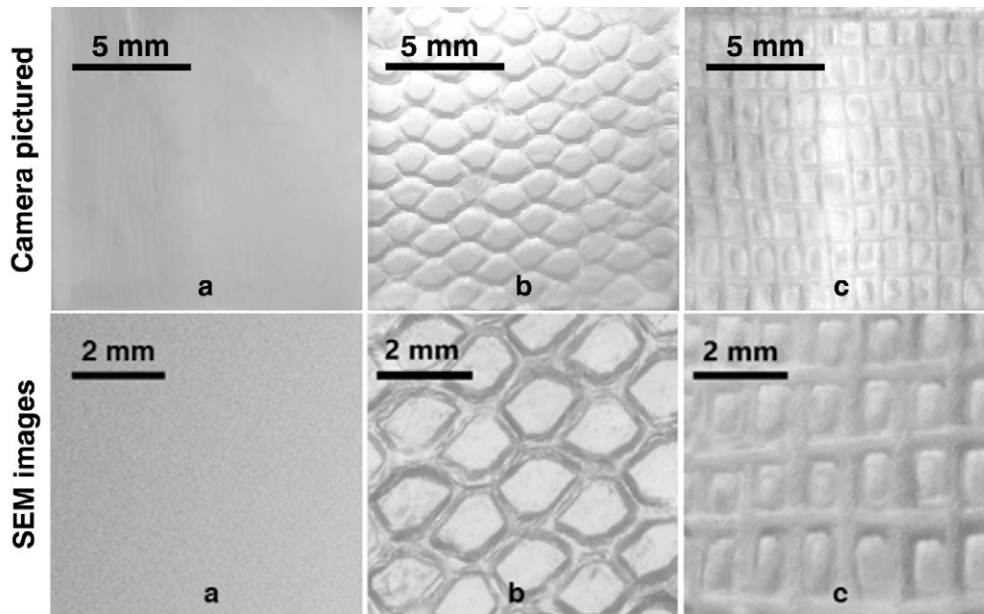
Fig. 4. Camera capture and SEM images from surface of fabricated layers, a: ONFS; b: PeTNFS; c: TeTNFS.
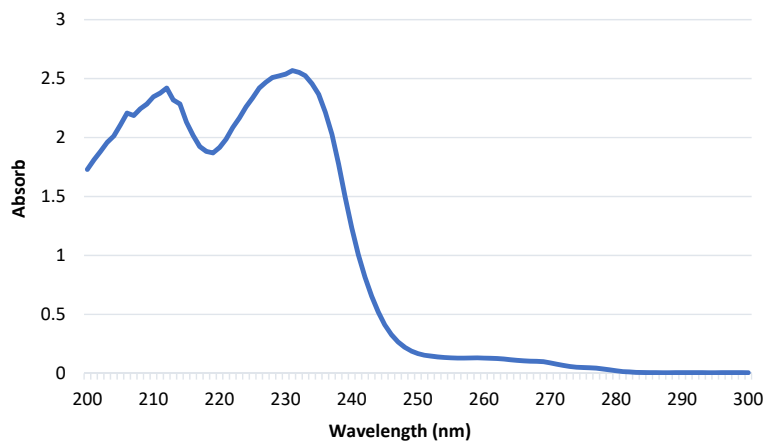

Fig. 5. Absorption spectrum of cetirizine in 200-300 nm.
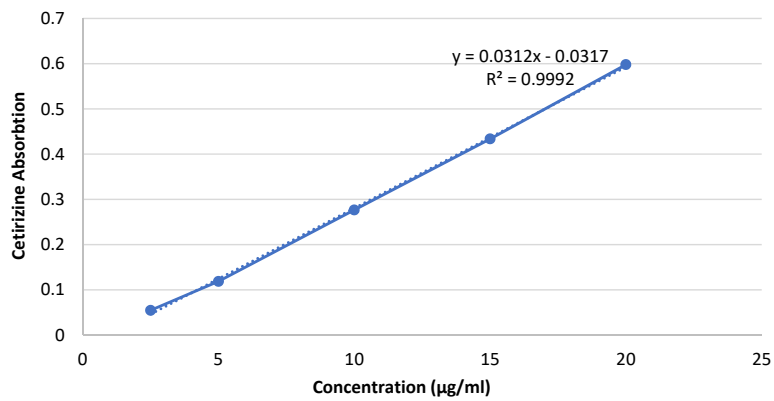

$y = 0.0312x - 0.0317$
$R^2 = 0.9992$

Fig. 6. Standard curve of cetirizine in 231 nm.

membrane, the amount of drug released can be calculated. According to the standard curve of cetirizine, initial weight of samples, applying the dilution factor (25 ml, Franz cell volume), the amount of released drug in PBS solution (due to the release of the drug from the nanofiber tissue) can be calculated. Finally, the drug release diagram based on time was plotted. This experiment was repeated 3 times for each sample and the results of drug release from each sample are shown in Fig. 8.

It was observed that the maximum drug release from ONFS was about 75% after 165 min; from PeTNFS, it was more than 98% after 150 min and from TeTNFS, it was more than 78% after 135 min.

Also, to calculate the drug release rate in the range in which the maximum drug release occurred, the slope of trendline equation of chart is equal to the rate of drug release. Trendline Equation of curves and Drug Release Rate are shown in Table 2. From the results, the rate of drug release in PeTNFS was more than that of other layers.

Drug release kinetics

Three usual kinetic models considered as zero-order model, first-order model and Higuchi model, and their matching with obtained releasing profiles were investigated. The diagram of release kinetic model for zero-order model is shown in Figs 8 and for the first-order model and Higuchi model shown in Fig. 9a and Fig. 9b respectively and the related results are shown in Table 3.

According to the results, the best fit for drug release kinetic of ONFS and TeTNFS samples were Higuchi model, it means the release of drugs from insoluble matrix as a square root of time dependent process based on Eq. (3), but it obeyed first order model for PeTNFS sample, meaning the release rate of drug from matrix is concentration dependent.

Fig. 7. Franz cell diffusion system.

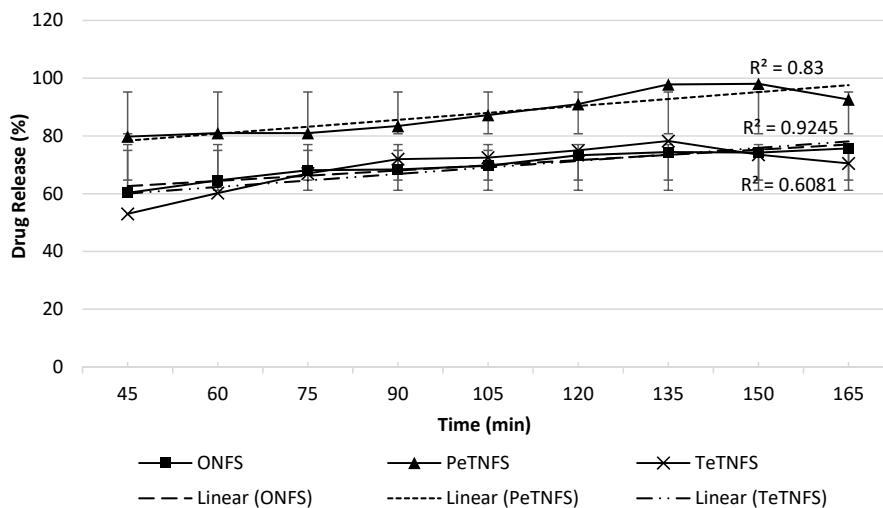Fig. 8. Drug release profile of cetirizine from different samples at different times and the related equations.

Table 2. Trendline equation of chart in Fig. 6 and drug release rate.

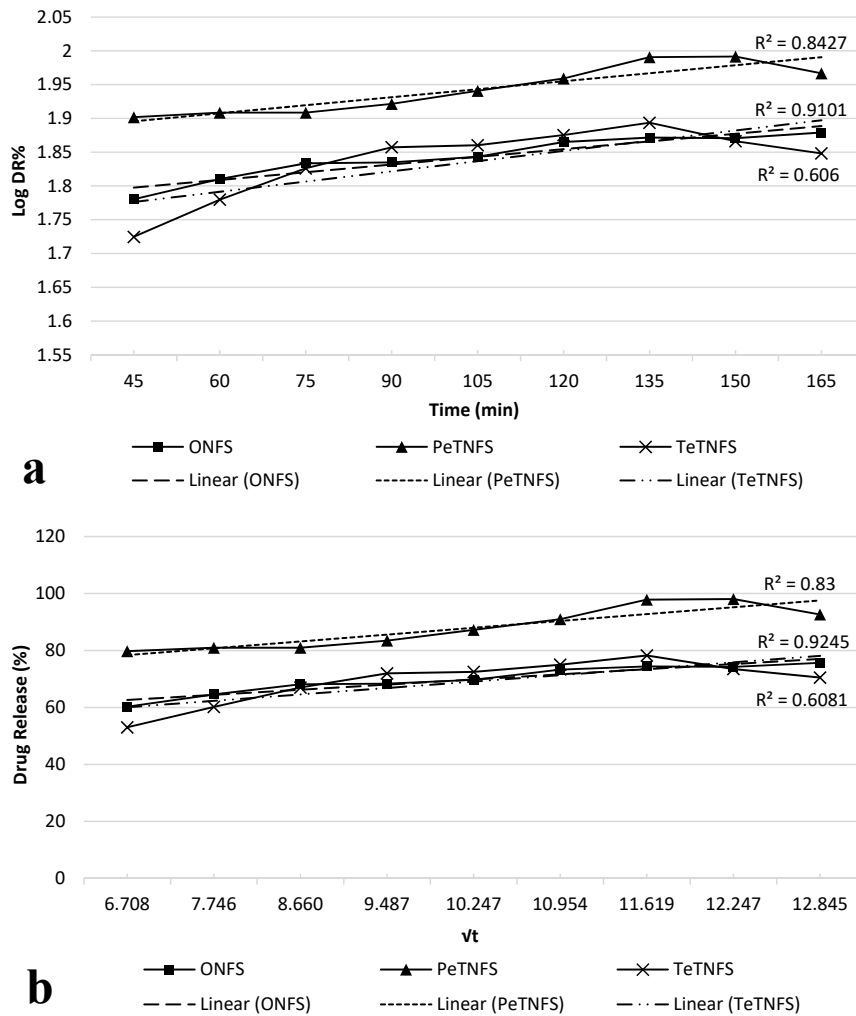| Sample	Trendline equation	Drug release rate
NFS	$y = 1.801x + 57.248$	1.801
NFS-R1	$y = 2.401x + 71.2$	2.401
NFS-R2	$y = 2.255x + 53.33$	2.255

Fig. 9: a: First order and b: Higuchi release model of cetirizine.

Table 3. R^2 value for samples in different kinetic models.

Sample	(R^2)Zero order	(R^2)First order	(R^2)Higuchi
NFS	0.925	0.910	0.956
NFS-R1	0.830	0.843	0.824
NFS-R2	0.608	0.606	0.689

The results of simulation of NFS effect on skin

The effect of ONFS, PeTNFS and TeNFS layers that was placed on dialysis film was studied and the morphology of dialysis film was investigated using SEM and shown in Fig. 10a, 10b and 10c respectively. Results show that the effect of PeTNFS on dialysis film (Fig. 10b) is clearly visible as compared to the other two samples. This effect is due to the shape of mesh and physical properties of the polymer.

Statistical Analysis

In Table 4, it is shown that P is greater than 0.05 (a significant level of 0.829). Therefore, the F statistic was used.

The most important table for analysis of variance is Table 5. In the first line, the significance level of the analysis of variance was considered (P <0.000). There is a significant difference between the sample, meaning there is at least, one uneven average among societies.
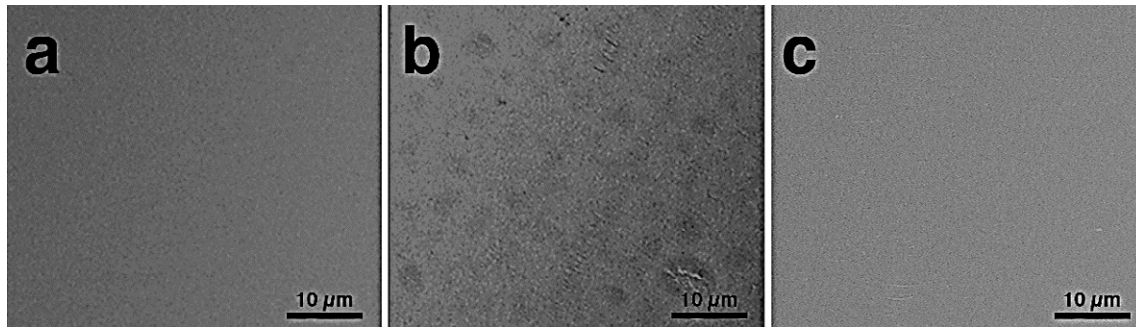
Fig.10: Effect of a: ONFS b: PeTNFS c: TeTNFS on dialysis film.

Table 4. Mauchly's Test of Sphericity.

Within Subjects Effect	Mauchly's W	Approx. Chi-Square	df	Sig.	Epsilon[b]		
					Greenhouse-Geisser	Huynh-Feldt	Lower-bound
Release	.963	.375	2	.829	.964	1.000	.500

Tests the null hypothesis that the error covariance matrix of the orthonormalized transformed dependent variables is proportional to an identity matrix.

a. Design: Intercept
Within Subjects Design: Release

b. May be used to adjust the degrees of freedom for the averaged tests of significance. Corrected tests are displayed in the Tests of Within-Subjects Effects table

Table 5. Tests of within-subjects effects.

	Source	Type III Sum of Squares	df	Mean Square	F	Sig.
Release	Sphericity Assumed	2704.394	2	1352.197	93.010	.000
	Greenhouse-Geisser	2704.394	1.929	1402.001	93.010	.000
	Huynh-Feldt	2704.394	2.000	1352.197	93.010	.000
	Lower-bound	2704.394	1.000	2704.394	93.010	.000
Error(Release)	Sphericity Assumed	319.842	22	14.538		
	Greenhouse-Geisser	319.842	21.218	15.074		
	Huynh-Feldt	319.842	22.000	14.538		
	Lower-bound	319.842	11.000	29.077		

Table 6. Pairwise comparisons.

(I) Release	(J) Release	Mean Difference (I-J)	Std. Error	Sig.[b]	95% Confidence Interval for Difference[b]	
					Lower Bound	Upper Bound
1	2	-16.867*	1.515	.000	-21.139	-12.595
	3	2.732	1.449	.258	-1.355	6.819
2	1	16.867*	1.515	.000	12.595	21.139
	3	19.599*	1.695	.000	14.818	24.380
3	1	-2.732	1.449	.258	-6.819	1.355
	2	-19.599*	1.695	.000	-24.380	-14.818

Based on estimated marginal means

*. The mean difference is significant at the .05 level.

b. Adjustment for multiple comparisons: Bonferroni.

From the comparison table below (Table 6), with a 95% confidence interval, the ONFS sample was compared with the TeTNFS sample, and it can be concluded that there is no significant difference between them, but the PeTNFS sample was significantly different from other samples.

CONCLUSION

This study aimed to fabricate nanofibrous scaffold (NFS) with an innovated electrospinning method called "Mesh electrospinning". Two non-conductive meshes with different patterns were used in mesh electrospinning to produce different

patterned surface with different morphology and roughness: one with pentagonal meshes and the other one with tetragonal meshes (PeTNFS and TeTNFS, respectively), and also, ordinary nanofibrous scaffold (ONFS) was fabricated. The spinning solution was prepared by dissolving 1.5 g nylon 6 in 5^{cc} formic acid (30% w/v) and the required amount of cetirizine (1% w/v) was added to this solution just before electrospinning. The electrospinning condition, voltage, distance and feed rate were chosen as 20 kV, 5 cm and 0.2 ml/h, respectively. After electrospinning, at first, the surface roughness of samples was measured. The roughness value for samples ONFS, PeTNFS and TeTNFS was 0.814, 4.163 and 2.292 μm, respectively. The nanofibrous scaffolds were used for *in-vitro* transdermal drug release test on dialysis film by Franz diffusion cell, and spectrophotometric method was used to determine the amount of drug released in phosphate buffer saline in pH 7.4. Also, the maximum wavelength absorbance of cetirizine was determined as λ_{max}=231 nm. Also, drug release kinetics was investigated. The best fit for drug release kinetic of ONFS and TeTNFS samples were Higuchi model but it obeyed first order model for PeTNFS sample. Afterwards, to simulate NFS effect on skin, NFS layers were placed on dialysis film, and after three hours, the morphology of skin was investigated by SEM and the effect of roughness from PeTNFS was clearly observed on dialysis film. Finally, according to statistical analysis, PeTNFS sample was significantly different from other samples. Therefore, mesh electrospinning method can increase and improve transdermal drug release properties.

CONFLICT OF INTEREST

The authors declare that there is no conflict of interests regarding the publication of this review article.

REFERENCES

1. Khajavi R., Abbasipour M., Bahador A., (2016), Electrospun biodegradable nanofibers scaffolds for bone tissue engineering. *J. Appl. Polym. Sci.* 133: 1-19.
2. Khajavi R., Abbasipour M., (2012), Electrospinning as a versatile method for fabricating coreshell, hollow and porous nanofibers. *Sci. Iran.* 19: 2029-2034.
3. Abbasipour M., Khajavi R., (2013), Nanofiber bundles and yarns production by electrospinning: A review. *Adv. Polym. Tech.* 32: 109-117.
4. Marsano E., Francis L., Giunco F., (2010), Polyamide 6 nanofibrous nonwovens via electrospinning. *J. Appl. Polym. Sci.* 117: 1754-1765.
5. Sencadas V., Correia D. M., Areias A., Botelho G., Fonseca, A. M., Neves I. C., Mendez S. L., (2012), Determination of the parameters affecting electrospun chitosan fiber size distribution and morphology. *Carbohyd. Polym.* 87: 1295-1301.
6. Camerlo A., Bühlmann-Popa A. M., Vebert-Nardin C., Rossi R. M., Fortunato G., (2014), Environmentally controlled emulsion electrospinning for the encapsulation of temperature-sensitive compounds. *J. Mater. Sci.* 49: 8154-8162.
7. Wang B., Wang Y., Yin T., Yu Q., (2010), Applications of electrospinning technique in drug delivery. *Chem. Eng. Commun.* 197: 1315-1338.
8. Chakraborty S., Liao I. C., Adler A., Leong K. W., (2009), Electrohydrodynamics: A facile technique to fabricate drug delivery systems. *Adv. Drug. Deliv. Rev.* 61: 1043-1054.
9. Kenawy E. R., Bowlin G. L., Mansfield K., Layman J., Simpson D. G., Sanders E. H., Wnek G. E., (2002), Release of tetracycline hydrochloride from electrospun poly (ethylene-co-vinylacetate), poly (lactic acid), and a blend. *J. Control Release.* 81: 57-64.
10. Prabaharan M., Jayakumar R., Nair S. V., (2011), Electrospun nanofibrous scaffolds-current status and prospects in drug delivery. *Adv. Polym. Sci.* 246: 241-262.
11. Zhang Y., Lim C. T., Ramakrishna S., Huang Z. M., (2005), Recent development of polymer nanofibers for biomedical and biotechnological applications. *J. Mater. Sci.* 16: 933-946.
12. Zamani M., Prabhakaran M. P., Ramakrishna S., (2013), Advances in drug delivery via electrospun and electrosprayed nanomaterials. *Int. J. Nanomed.* 8: 2997-3017.
13. Boland E. D., Wnek G. E., Simpson D. G., Pawlowski K. J., Bowlin G. L., (2001), Tailoring tissue engineering scaffolds using electrostatic processing techniques: A study of poly (glycolic acid) electrospinning. *J. Macromol. Sci. A.* 38: 1231-1243.
14. Yang F., Murugan R., Wang S., Ramakrishna S., (2005), Electrospinning of nano/micro scale poly (L-lactic acid) aligned fibers and their potential in neural tissue engineering. *Biomater.* 26: 2603-2610.
15. Matthews J. A., Wnek G. E., Simpson D. G., Bowlin G. L., (2002), Electrospinning of collagen nanofibers. *Biomacromolec.* 3: 232-238.
16. Min B. M., Lee G., Kim S. H., Nam Y. S., Lee T. S., Park W. H., (2004), Electrospinning of silk fibroin nanofibers and its effect on the adhesion and spreading of normal human keratinocytes and fibroblasts in vitro. *Biomater.* 25: 1289-1297.
17. Huang Y., Onyeri S., Siewe M., Moshfeghian A., Madihally S. V., (2005), In vitro characterization of chitosan–gelatin scaffolds for tissue engineering. *Biomater.* 26: 7616-7627.
18. Khil M. S., Cha D. I., Kim H. Y., Kim I. S., Bhattarai N., (2003), Electrospun nanofibrous polyurethane membrane as wound dressing. *J. Biomed. Mater. Res. B.* 67: 675-679.
19. Ignatova M., Manolova N., Markova N., Rashkov I., (2009), Electrospun non-woven nanofibrous hybrid mats based on chitosan and PLA for wound-dressing applications. *Macromol. Biosci.* 9: 102-111.
20. Zhang N., Deng Y., Tai Q., Cheng B., Zhao L., Shen Q., He R., Hong L., Liu W., Guo S., Liu K., (2012), Electrospun TiO$_2$ nanofiber-based cell capture assay for detecting circulating tumor cells from colorectal and gastric cancer patients. *Adv. Mater.* 24: 2756-2760.

21. Hou S., Zhao L., Shen Q., Yu J., Ng C., Kong X., Wu D., Song M., Shi X., Xu X., Ou Yang W. H., (2013), Polymer nanofiber-embedded microchips for detection, isolation, and molecular analysis of single circulating melanoma cells. *Angew. Chem. Int. Edit.* 52: 3379-3383.

22. Zhao L., Lu Y. T., Li F., Wu K., Hou S., Yu J., Shen Q., Wu D., Song M., OuYang W. H., Luo Z., (2013), High-purity prostate circulating tumor cell isolation by a polymer nanofiber-embedded microchip for whole exome sequencing. *Adv. Mater.* 25: 2897-2902.

23. Zong X., Kim K., Fang D., Ran S., Hsiao B. S., Chu B., (2002), Structure and process relationship of electrospun bioabsorbable nanofiber membranes. *Polymer.* 43: 4403-4412.

24. Kenawy E. R., Bowlin G. L., Mansfield K., Layman J., Simpson D. G., Sanders E. H., Wnek G. E., (2002), Release of tetracycline hydrochloride from electrospun poly (ethylene-co-vinylacetate), poly (lactic acid), and a blend. *J. Control Release.* 81: 57-64.

25. Xie J., Wang C. H., (2006), Electrospun micro-and nanofibers for sustained delivery of paclitaxel to treat C6 glioma in vitro. *Pharm. Res.* 23: 1817-1822.

26. Mano J. F., (2008), Stimuli-responsive polymeric systems for biomedical applications. Adv. Eng. Mater. 10: 515-527.

27. Alvarez-Lorenzo C., Concheiro A., (2014), Smart drug delivery systems: From fundamentals to the clinic. *Chem. Commun.* 50: 7743-7765.

28. Vaquette C., Cooper-White J. J., (2011), Increasing electrospun scaffold pore size with tailored collectors for improved cell penetration. *Acta Biomater.* 7: 2544-2557.

29. Wu Y., Dong Z., Wilson S., Clark R. L., (2010), Template-assisted assembly of electrospun fibers. *Polymer.* 51: 3244-3248.

30. Zhang D., Chang J., (2008), Electrospinning of three-dimensional nanofibrous tubes with controllable architectures. *Nano Lett.* 8: 3283-3287.

31. Wang Y., Wang G., Chen L., Li H., Yin T., Wang B., Lee J. C., Yu Q., (2009), Electrospun nanofiber meshes with tailored architectures and patterns as potential tissue-engineering scaffolds. *Biofabric.* 1: 015001-015006.

32. Saadatmand M. M., Yazdanshenas M. E., Khajavi R., Mighani F., Toliyat T., (2017), Templated roughness on the surface of polyamide nanofibrous mat by mesh electrospinning. *Orient. J. Chem.* 33: 2356-2562.

33. Verma J., Khandelwal A., (2016), Synthesis of silica nanoparticles and its potential for drug delivery. *Int. J. Biochem. Biotechnol. Biomed. Sci.* 2: 181-186.

34. Chatzēiōannou T. P., (1993), Quantitative calculations in pharmaceutical practice and research (pp. 345-348). New York: *John Wiley & Sons.*

35. Bourne D. W. A., (2002), Pharmacokinetics. In: Banker GS, Rhodes CT, Modern Pharmaceutics, 4th edition (pp. 67-92). New York: *Marcel Dekker Inc.*

36. Higuchi T., (1963), Mechanism of sustained-action medication. Theoretical analysis of rate of release of solid drugs dispersed in solid matrices. *J. Pharm. Sci.* 52: 1145-1149.

37. Chauhan N. P. S., Meghwal K., Juneja P., Chaudhary J., Chandra Meghwal R., Punjabi P. B., (2015), Controlled release: Porous polymer application. In encyclopedia of biomedical polymers and polymeric biomaterials (pp. 2155-2172). New York: *Taylor and Francis.*

38. Ho H. O., Huang F. C., Sokoloski T. D., Sheu M. T., (1994), The influence of cosolvents on the in-vitro percutaneous penetration of diclofenac sodium from a gel system. *J. Pharm. Pharmacol.* 46: 636-642.

39. Khan M. I., Murtaza G., Sher M., Iqbal M., Waqas M. K., Rasool A., Fatima U., Asad M. H., Kahlid A., Usman F., Najam-Us-Saqib Q., (2011), Development and validation of stability indicating assay method of cetirizine hydrochloride by HPLC. *Afr. J. Pharm. Pharmacol.* 5: 143-149.

40. Sultana N., Arayne M. S., Shamshad H., (2010), In vitro studies of the interaction between cetirizine and H 2 receptor antagonists using spectrophotometry and reversed-phase high-performance liquid chromatography. *Med. Chem. Res.* 19: 462-474.